IEEE Access
Multidisciplinary | Rapid Review | Open Access Journal

Received 29 May 2023, accepted 1 July 2023, date of publication 10 July 2023, date of current version 18 July 2023.

Digital Object Identifier 10.1109/ACCESS.2023.3293489

RESEARCH ARTICLE

Beamforming for NOMA Under Similar Channel Conditions Including Near-Field Formulation

ÁLVARO PENDÁS-RECONDO, RAFAEL GONZÁLEZ AYESTARÁN, (Senior Member, IEEE), AND JESÚS ALBERTO LÓPEZ-FERNÁNDEZ

Group of Signal Theory and Communications, Department of Electrical Engineering, University of Oviedo, 33203 Gijón, Spain

Corresponding author: Álvaro Pendás-Recondo (pendasalvaro@uniovi.es)

This work was supported in part by Ministerio de Ciencia e Innovación and Agencia Estatal de Investigación (MICIN)/(AEI)/10.13039/501100011033 within Project PID2020-114172RBC21 (ENHANCE-5G), and in part by Gobierno del Principado de Asturias under Project SV-PA-21 AYUD/2021/51706 and "Severo Ochoa" Program Grant PA-22-BP21-116.

ABSTRACT Non-Orthogonal Multiple Access (NOMA) has emerged as a promising strategy for increasing spectral efficiency in wireless multiuser communications. The performance of NOMA highly depends on the users' channel conditions, being enhanced when these are significantly different, i.e., one strong user and one weak user. On the contrary, rate fairness is compromised when users present similar channel conditions since the maximization of the sum capacity may result in the allocation of most resources to one user. In general, this problem can be avoided with correct user grouping. However, there are scenarios, e.g., picocells or femtocells, where finding users with distinctive channel conditions is not always possible. In this paper, we study the application of beamforming in a two-user Multiple-Input-Single-Output (MISO) downlink NOMA system to achieve rate fairness through channel shaping even when the conditions of both users are similar. The proposed formulation includes the effect of Near-Field (NF) radiation, which yields an accurate modeling of the problem at hand in a small-cell scenario. We use an optimization algorithm to jointly calculate both the power allocation and the complex weights to be applied to the elements of a given array. Numerical simulations across scenarios with distinctive or similar channel conditions show that the proposed approach outperforms alternative NOMA methods in ensuring rate fairness. Additionally, it yields improved overall rates compared to Far-Field (FF) formulation-based modelling and beamforming Time Division Multiple Access (TDMA) solutions.

INDEX TERMS Beamforming, multiple-input-single-output (MISO), near-field (NF), non-orthogonal multiple access (NOMA), power allocation, rate fairness.

I. INTRODUCTION

Non-Orthogonal Multiple Access (NOMA) has emerged as a crucial component for the present and future of fifth generation (5G) wireless mobile communications [1], mainly due to its spectral efficiency [2] and performance in terms of outage [3]. The key features of 5G are reduced latency, high connectivity, and ultra-fast speed. However, as the number of devices connected to the network grows exponentially, simultaneous access and aggregate capacity become critical challenges. To address these issues, Multiple Access (MA) division strategies in time, Time Division Multiple Access (TDMA), frequency (FDMA) and code (CDMA) can be supplemented with the NOMA power/code division. NOMA combines Superposition Coding (SC) with Successive Interference Cancellation (SIC) to offer additional multiplexing in an already occupied slot.

The performance of NOMA can be enhanced by incorporating spatial diversity in Multiple-Input Multiple-Output (MIMO) systems [4]. Joint optimization of user power allocation and beamforming is a challenging task that has been studied recently [5], [6], [7], [8], [9], [10], [11], [12], [13]. Other challenges related to NOMA include imperfect SIC and user grouping. Imperfect SIC degrades the system by causing error propagation and negatively affecting the obtained rates [14]. User grouping (or pairing, for two users) studies how to choose the users that apply NOMA in a network, which significantly impacts its performance [12], [15], [16],

The associate editor coordinating the review of this manuscript and approving it for publication was Yafei Hou.

[17], [18]. It has been shown that, in general, selected users should have significantly different channel conditions [17]. This allows different levels of allocated power for each user, which improves SIC without an impact on rate fairness [19]. However, in scenarios with only two users and similar channel conditions, such as in a picocell or femtocell, optimizing the system sum rate can result in allocating most resources to one user at the expense of the other [18]. In such conditions, if all users are in the same Quality of Service (QoS) category and rate fairness is essential, NOMA's performance may be inferior to that of other MA techniques. Another challenge that arises in small-cell scenarios is that, depending on the distances involved and the operating frequency, the antenna might radiate in the Near-Field (NF) [20], [21]. Consequently, incorporating this effect into the problem formulation enhances the accuracy of the model and the reliability of the solutions.

In this paper, we investigate the application of beamforming in a two-user Multiple-Input-Single-Output (MISO) downlink NOMA system across various scenarios, showing its ability to overcome the limitations of Single-Input Single-Output (SISO) NOMA when both users have similar channel conditions. We consider the typical NOMA case where the user performing SIC has a significantly stronger channel, as well as cases where both users have comparable channel conditions, which may occur in 5G indoor settings. Our formulation includes the effect of imperfect SIC, as proposed in [14], and NF radiation.

The design of MIMO and MISO NOMA systems when users have similar channel conditions has been considered in the literature before. In [22], the authors investigate the MIMO case in the context of small-packet transmission for the Internet of Things (IoT). However, it is assumed that one user has priority, and as a result, enjoys a higher Quality of Service (QoS) compared to the other user. This leads to solving the problem by selecting maximum beamforming for the main user, while power allocation is left as a degree of freedom to adjust the system. The same beamforming strategy is proposed in [23], where multicast-unicast streaming is considered, i.e., the primary user is interested in both its private message and the multicast message received by the secondary user. In contrast, a different scenario is considered in this paper, where both users belong to the same QoS category, i.e, their final rates are equally important, and each user is only interested in its intended message.

The main contributions of this paper can be summarized as follows:

- We show that MISO beamforming adds an extra degree of freedom through channel shaping and thus can solve the problem of single-antenna NOMA where two users have similar channel conditions. We include in our formulation the effect of imperfect SIC and NF conditions. To the best of our knowledge, there is no previous work that considers the specific case of NF beamforming for NOMA.
- In contrast to prior studies investigating NOMA under similar channel conditions [22], [23], our research examines a different scenario in which both users fall under the same QoS category and are solely focused on receiving their intended messages.
- In order to prove the value of our model, we conducted performance evaluations where we show that our approach outperforms other alternatives in the given context.
- Additionally, to demonstrate the performance of MISO NOMA in seemingly unfavorable scenarios and the presence of non-idealities, we present a representative comparison with beamforming TDMA. The numerical experiments carried out in this work show that NOMA outperforms TDMA when the interference cancellation level is sufficiently high.
- Finally, our formulation of the problem considers specific antenna array features, defined by its geometry and the radiation patterns of its elements, thereby increasing its practical applicability in real-world situations. Besides, the proposed algorithm incorporates a power allocation constraint as input that would ensure correct SIC performance given a particular system configuration.

While our formulation outlines the joint power allocation and beamforming optimization problem, our research does not primarily focus on identifying the best strategies to tackle it. A representative example of this effort for a downlink two-user scenario can be found in [6], where a non-convex problem with non-linear constraints, similar to the one we face, is transformed into a convex one under certain assumptions. However, our formulation exhibits notable differences, as we incorporate imperfect SIC and NF conditions and strive to ensure rate fairness in every scenario. We leave it to future work to explore various optimization strategies that could enhance the robustness and efficiency of the proposed algorithm.

The rest of the paper is organized as follows. The system model and problem formulation are described in Section II. Section III describes the optimization problem and its upper bounds. The performance evaluation through simulations of the proposed method is presented in Section IV. Finally, conclusions are drawn in Section V.

Notation: h, $\mathbf{h}$ and $\mathbf{H}$ denote a scalar, column vector and matrix, respectively. $(\cdot)^T$ and $(\cdot)^H$ denote transpose and conjugate transpose (or hermitian), respectively. $|\cdot|$ denotes the absolute value, $\|\cdot\|$ refers to the $\ell 2$-norm and $\mathbb{E}\{\cdot\}$ to the expected value. The real and imaginary parts of a complex number, x, are denoted by $\Re(x)$ and $\Im(x)$, respectively. A three-dimensional position vector in cartesian coordinates is represented as $\vec{r}$. In addition, dot product between two arbitrary position vectors, $\vec{r}_1$ and $\vec{r}_2$, is noted as $\vec{r}_1 \cdot \vec{r}_2$.

II. SYSTEM MODEL

A. SINGLE-INPUT-SINGLE-OUTPUT NOMA

Let us consider a basic downlink NOMA scenario with one Base Station (BS), where only two users are assigned to a group or cluster to perform NOMA [15], [16], [17], [18]. The scenario is represented in Fig. 1. Typically, the user with a weaker channel is allocated a higher transmission power [3], whereas the user with the stronger channel implements a SIC scheme at the receiver in order to recover its data from the superimposed signal. We initially consider the SISO case, denoting h_i as the complex channel coefficient between the BS and the i-th user, $i = 1, 2$; n_i as the additive white Gaussian noise with zero mean and variance $\sigma_{n_i}^2$,

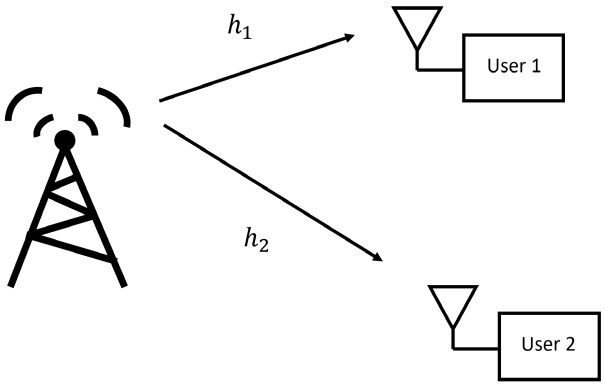

FIGURE 1. Illustration of a NOMA downlink scenario with one Base Station and two users.

$n_i \sim \mathcal{CN}\left(0, \sigma_{n_i}^2\right)$; and p_i as the allocated power. We initially assume $|h_1| > |h_2|$ and consequently $p_2 > p_1$. The received signal at each user y_i after SIC is performed by user 1 can be expressed as

$$\begin{cases} y_1 = \sqrt{p_1} h_1 x_1 + \beta\sqrt{p_2} h_1 x_2 + n_1 \\ y_2 = \sqrt{p_2} h_2 x_2 + \sqrt{p_1} h_2 x_1 + n_2 \end{cases} \tag{1}$$

where x_i is the transmitted symbol to the i-th user, $\mathbb{E}\{|x_1|^2\} = \mathbb{E}\{|x_2|^2\} = 1$; and β, $0 \leq \beta \leq 1$, is the interference cancellation factor, accounting for a potentially imperfect SIC, $\beta = 0$ corresponding to perfect cancellation and $\beta = 1$ to fully incorrect cancellation [14]. Considering the transmission of Proper Gaussian Signals (PGS) [24], we have the well-known expression of the capacity for each user, adding the imperfect SIC term for user 1 [14]:

$$\begin{cases} R_1 = \log_2\left(1 + \dfrac{p_1 |h_1|^2}{\sigma_{n_1}^2 + \beta^2 p_2 |h_1|^2}\right) \\ R_2 = \log_2\left(1 + \dfrac{p_2 |h_2|^2}{\sigma_{n_2}^2 + p_1 |h_2|^2}\right). \end{cases} \tag{2}$$

Note that (2) refers to the channel capacity for users 1 and 2 that, under the considered scenario, equals the rate achieved by each one, which explains the notation R_i.

Since user 1 performs SIC, it has to first decode the message intended for user 2, x_2. As stated in [3], there is an implicit condition of $R_1^{(2)} > R_2$, where $R_1^{(2)}$ denotes the rate of user 1 to decode the message intended for user 2 and can be expressed as [5]

$$R_1^{(2)} = \log_2\left(1 + \frac{p_2 |h_1|^2}{\sigma_{n_1}^2 + p_1 |h_1|^2}\right). \tag{3}$$

Nonetheless, the condition of $R_1^{(2)} > R_2$ does not guarantee perfect SIC; it merely indicates that it must occur at user 1. While it is true that SIC performance, measured in terms of β, is generally improved with the increase of $R_1^{(2)}$, it is also influenced by the system setting and realization [25].

Additionally, when considering SIC there are some boundaries for the power allocation depending on the modulation used by both users as studied in [26] and [27], which imposes a minimum ratio of $\frac{p_2}{p_1}$. Considering $p_2 = ap_1$, where we denote a as the power allocation factor, this constraint can be expressed as $\frac{p_2}{p_1} \geq a_{\min} \geq 1$.

A higher value of $\frac{p_2}{p_1}$ has three impacts: firstly, it ensures the constraint of $\frac{p_2}{p_1} \geq a_{\min}$ is met; secondly, it augments $R_1^{(2)}$, thereby improving SIC performance; and finally, it also enhances R_2, which can be inferred from equation (2). In the interference-limited case, these rates that we denote as $R_{\text{i.l.2}}$ and $R_{\text{i.l.1}}^{(2)}$, where $p_1 |h_2|^2 \gg \sigma_{n_2}^2$ and $p_1 |h_1|^2 \gg \sigma_{n_1}^2$ respectively, are given by

$$R_{\text{i.l.2}} \approx R_{\text{i.l.1}}^{(2)} \approx \log_2\left(1 + \frac{p_2}{p_1}\right) = \log_2(1 + a) \tag{4}$$

where the Signal-to-Interference plus Noise Ratio (SINR) in both terms is approximated by $\frac{p_2}{p_1} = a$.

Although power allocation is controlled, its conditions are preceded by the assumption of $|h_1| > |h_2|$, which is often considered without loss of generality [6], as long as user allocation for NOMA is performed properly [12], [15], [16], [17], [18]. Nevertheless, there are some scenarios where it can be compromised, e.g., cells with few users and time-variant channels where it is not trivial to order them according to their channel conditions. A more specific example is a cluster with only two users where $|h_1| \approx |h_2|$. In that scenario, and continuing with the assumption that SIC is implemented at user 1, it remains essential to uphold the condition $\frac{p_2}{p_1} \geq a_{\min} \geq 1$ to ensure effective SIC performance. However, a high ratio of $\frac{p_2}{p_1}$ translates into an uneven rate split in favor of user 2 since it is allocated higher power even under similar channel conditions. Consequently, rate fairness is not achieved. For example, let us set $p_1 = 1$ mW, $p_2 = 10$ mW, $h_1 = h_2 = 1$, $\sigma_{n_{1,2}}^2 = 1$ mW, and $\beta = 0$. According to (2) the resulting capacities would be $R_1 = 1$ bps/Hz and $R_2 = 2.58$ bps/Hz being R_2 much greater even when assuming perfect SIC. From now on, we will continue to denote user 1 as the one that is performing SIC as expressed in (1) and (2) while considering the scenario where $|h_1| \approx |h_2|$ (Section IV).

B. NOMA WITH BEAMFORMING IN NEAR-FIELD

The combination of NOMA and beamforming provides an extra degree of freedom to deal with channel constraints. Let us now consider the MISO case when the BS has an array of N different antennas that are used for controlling its radiation pattern through beamforming. This means that the same signal is transmitted by the N antennas except for a complex weight factor. The rate expressions after SIC can be now written as

$$\begin{cases} R_1 = \log_2\left(1 + \dfrac{p_1 g_1}{\sigma_{n_1}^2 + \beta^2 p_2 g_1}\right) \\ R_2 = \log_2\left(1 + \dfrac{p_2 g_2}{\sigma_{n_2}^2 + p_1 g_2}\right) \end{cases} \tag{5}$$

where g_i the effective gain of the array, which includes channel propagation losses and beamforming gain at the position

of the i-th user,

$$g_i = \left| \sum_{n=1}^{N} w_n h_{i,n} \right|^2 = \left| \mathbf{w}^T \mathbf{h}_i \right|^2 \tag{6}$$

where the vector $\mathbf{w}$ contains the weights, $w_n \in \mathbb{C}$, each applied to the n-th element of the array, and $\mathbf{h}_i$ is the vector containing the complex channel coefficients between each element of the array and the i-th user, $h_{i,n}$. Assuming free space conditions, NF formulation for the array, but a distance far enough between the BS and the users to consider each individual element of the array in the Far-Field (FF) region [28], we have [29]:

$$h_{i,n} = \frac{\lambda \sqrt{f_{i,n}(\vec{r}_i, \vec{r}\,'_n)} e^{-jk\|\vec{r}_i - \vec{r}\,'_n\|}}{4\pi \|\vec{r}_i - \vec{r}\,'_n\|} \tag{7}$$

where $\vec{r}_i$ is the position vector of the i-th user, and $\vec{r}\,'_n$ is the position vector of the n-th element of the array. The wave number is denoted as $k = 2\pi/\lambda$, being λ the wavelength. Finally, $f_{i,n}(\vec{r}_i, \vec{r}\,'_n)$ is the product of the transmit and receive antenna field radiation patterns between the n-th element of the array and the i-th user. More complex models of the antenna array radiation can be included in this formulation by modifying (7), e.g., coupling effects between the elements in the antenna array as long as the coupling matrix, $\mathbf{M}$ [30], is well-characterized, substituting $\mathbf{h}_i$ by $\mathbf{s}_i = \mathbf{M}\mathbf{h}_i$.

Note that the general NOMA condition of $|h_1| > |h_2|$ is transformed into $g_1 > g_2$, and all the expressions derived in Section II-A remain valid substituting $|h_i|^2$ by g_i. The approach presented in this section gives an extra degree of freedom compared to SISO NOMA since in the MISO case it is possible to modify g_1 and g_2 through the array weight vector $\mathbf{w}$.

Let us now compare NF versus FF formulation. Denoting D as the largest dimension of the array, and d as the distance between its center and a given point in the space, the reactive NF region outer boundary is commonly taken as $d_{\mathrm{RNF}} < 0.62\sqrt{(D^3/\lambda)}$ [31] and the outer boundary for the NF region is $d_{\mathrm{NF}} < 2D^2/\lambda$. The FF region is found for $d > d_{\mathrm{NF}}$, where it is considered that the angular field distribution is not dependent upon the distance from the antenna, approximating the distance terms in (7) by $\|\vec{r}_i - \vec{r}\,'_n\| \approx \|\vec{r}_i\|$ in the amplitude, and $\|\vec{r}_i - \vec{r}\,'_n\| \approx \|\vec{r}_i\| - \vec{r}\,'_n \cdot \hat{r}_i$ in the phase, being $\hat{r}_i = \frac{\vec{r}_i}{\|\vec{r}_i\|}$, which yields

$$h_{i,n,\mathrm{FF}} \approx \frac{\lambda \sqrt{f_{i,n}(\vec{r}_i, \vec{r}\,'_n)} e^{-jk(\|\vec{r}_i\| - \vec{r}\,'_n \cdot \hat{r}_i)}}{4\pi \|\vec{r}_i\|}. \tag{8}$$

In Section IV, we show how the proposed NF formulation improves the resulting rates compared with the FF approximation when $d < d_{\mathrm{NF}}$. Lastly, the effective gain can be expressed as the product of two terms:

$$g_i = g_{i,\mathrm{BF}}\, g_{i,\mathrm{NB}} \tag{9}$$

where $g_{i,\mathrm{BF}}$ is the beamforming gain and $g_{i,\mathrm{NB}}$ is the effective gain in the non-beamforming (or SISO) case, in which a single antenna at the center of the array transmits all the power. The effective gain at the position of i-th user for the single antenna case, $g_{i,\mathrm{BF}} = 1$, may be just expressed as: $g_i = g_{i,\mathrm{NB}} = |h_i|^2$. In that case, the term $|h_i|^2$ incorporates the antenna gain in the direction of the i-th user as a part of the channel propagation losses. This aspect is similarly included for each element of the array in $h_{i,n}$ in equation (7) by the term $f_{i,n}(\vec{r}_i, \vec{r}\,'_n)$. In this manner, by examining $g_{i,\mathrm{BF}}$, we can assess the impact of beamforming on channel capacity and more effectively demonstrate the proposed technique's capability to concentrate the radiated power from the BS at the users' locations compared with the SISO case (Section IV).

III. OPTIMIZATION PROBLEM

A. PROBLEM DESCRIPTION

Given a scenario characterized by N, $\mathbf{h}_1$, $\mathbf{h}_2$, $\sigma^2_{n_1}$, $\sigma^2_{n_2}$ and β, it is possible to find the optimum set of weights, $\mathbf{w}_{\mathrm{opt}}$, and power allocation factor, a_{opt}, which jointly maximize a goal function of R_1 and R_2, which, from now on, we will denote as R. Power allocation by itself introduces a degree of freedom, but it is subject to certain limitations. Firstly, as explained in Section II-A, the condition $\frac{p_2}{p_1} \geq a_{\min} \geq 1$ must be met to ensure SIC performance, with $a_{\min}$ depending on the system realization and chosen modulation. Second, the power budget imposes that $p_1 + p_2 = p_{\max}$. For the beamforming scenario this constraint translates to $(p_1 + p_2)\|\mathbf{w}\|^2 = p_{\max}$. For the sake of simplicity, we adopt the assumption of $\|\mathbf{w}\|^2 = 1$, which yields:

$$p_1 = \frac{p_{\max}}{1+a} = \frac{p_2}{a}. \tag{10}$$

An upper bound for a, $a_{\max}$, can be defined as the power allocation factor that yields the minimum power for user 1. We propose an expression for its calculation in Section III-B. In addition, there is a constraint related to the maximum input power for each element of the array, that is $(p_1 + p_2)\,|w_n|^2 \leq p_{n,\max}$.

To achieve rate fairness, we adopt the strategy of maximizing the geometric mean of the capacities, $R = \sqrt{R_1 R_2}$, which is equivalent to maximizing the product of both rates as proposed in [5]. Consequently, the joint power allocation and beamforming optimization problem can be described as:

$$\begin{aligned} \max_{a,\mathbf{w}} \quad & R = \sqrt{R_1 R_2} \\ \text{s.t.} \quad & a_{\min} \leq a \leq a_{\max} \\ & \|\mathbf{w}\|^2 \leq 1 \\ & p_{\max}\,|w_n|^2 \leq p_{n,\max} \end{aligned} \tag{11}$$

which yields a non-convex optimization problem with non-linear constraints, where each constraint can be expressed as an inequality. Defining a vector $\mathbf{x}$ of $2N+1$ real variables that contain both real and imaginary parts of $\mathbf{w}$, as well as the power allocation factor a, $\mathbf{x} = [\,\Re(\mathbf{w}),\, \Im(\mathbf{w}),\, a\,]$, the optimization problem can be rewritten using Lagrange multipliers [32] as:

$$\mathcal{L}(\mathbf{x}, \boldsymbol{\lambda}) = R(\mathbf{x}) - \sum_{i=1}^{N+3} \lambda_i c_i(\mathbf{x}) = R(\mathbf{x}) - \boldsymbol{\lambda}\mathbf{c}(\mathbf{x}) \tag{12}$$

where $\boldsymbol{\lambda}$ is the vector containing the λ_i Lagrange multipliers corresponding to the $N+3$ inequality constraints expressed in $\mathbf{c}(\mathbf{x})$, each $c_i(\mathbf{x}) \leq 0$. Noting that information about $\mathbf{w}$

corresponds to the first $2N$ elements of $\mathbf{x}$, while a is at the $(2N+1)$-th position, each constraint can be defined as:

$$\begin{aligned} c_n(x_n, x_{n+N}) &= p_{\max} |w_n|^2 - p_{n,\max} \\ & \qquad n = 1, 2, \cdots N \\ c_{N+1}(x_1, x_2, \cdots x_{2N}) &= \|\mathbf{w}\|^2 - 1 \\ c_{N+2}(x_{2N+1}) &= a_{\min} - a \\ c_{N+3}(x_{2N+1}) &= a - a_{\max}. \end{aligned} \tag{13}$$

where $|w_n|^2 = x_n^2 + x_{n+N}^2$, $\|\mathbf{w}\|^2 = \sum_{n=1}^{2N} x_n^2$ and $a = x_{2N+1}$.

The restructured optimization problem can be tackled using the Sequential Quadratic Programming (SQP) algorithm [33], which seeks to fulfill the Karush-Kuhn-Tucker (KKT) conditions at every step of the process. We leave as future work a more in-depth study of the optimization problem that increases its robustness and efficiency, e.g., by discomposing it in smaller problems that can be converted to convex. Examples of similar studies can be found in [5], [6], [7], [8], [9], [10], [11], [12], and [13].

B. UPPER BOUNDS

A more careful analysis of the problem conditions allows us to define some upper bounds for the maximum capacities. It should be noted that the highest possible value of g_i for the i-th user is given by the solution of the MISO beamforming problem [34]. Consequently, the upper bound for g_i, $g_{i\max}$, is obtained when $\mathbf{w}^T = \frac{\mathbf{h}_i^H}{\|\mathbf{h}_i\|}$, yielding $g_{i\max} = \|\mathbf{h}_i\|^2$ which maintains the constraint of $\|\mathbf{w}\|^2 = 1$. It is clear that simultaneously obtaining $g_{1\max}$ and $g_{2\max}$ is only possible in very specific scenarios. For any given power allocation factor, these values define an upper bound for both effective gains. Since both capacity expressions, $R_1(g_1)$ and $R_2(g_2)$ are strictly increasing, this analysis also yields the values of $R_{1\max}$ and $R_{2\max}$, which represent the upper bound for R_1 and R_2.

Having established the upper bound for g_1, it is possible to select criteria for defining the maximum value of the power allocation factor, $a_{\max}$. This value results in the minimum power for user 1 as stated in (10), which we denote as $p_{1\min}$. We establish this bound for the scenario in which, even with perfect cancellation ($\beta = 0$) and $g_{1\max}$, the SINR for R_1 equals 1. That is, according to (5) and (10), $\frac{p_{1\min} g_{1\max}}{\sigma_{n_1}^2} = 1$, which yields $a_{\max} = \frac{p_{\max} g_{1\max}}{\sigma_{n_1}^2} - 1$. Other criteria could also be considered for this purpose.

IV. PERFORMANCE EVALUATION

In this section, we present simulated results for a square planar antenna array that consists of 12×12 isotropic elements, $N = 144$. The array is arranged on the XY plane, with its center located at the origin $\vec{r} = (0, 0, 0)$. The distance between the centers of the elements is set to 0.63λ. Two different scenarios are considered: one in which the channel for user 1 is significantly stronger than for user 2, as it is typical for NOMA, and another in which both users experience similar channel conditions. Although most results depend on λ and can be applied to any frequency, we provide a specific example using the 2.4 GHz band, where $\lambda = 0.125$ m. Considering the distances defined in Section II-B (D, d_{RNF} and d_{NF}) and 2.4 GHz as working frequency, we get that the largest dimension of the antenna array, D, is approximated by $D \approx 0.63 \times 11\lambda \approx 0.87$ m; the reactive NF region is $d_{\text{RNF}} < 0.62\sqrt{(D^3/\lambda)} \approx 11.31\lambda \approx 1.41$ m; and $d_{\text{NF}} < 2D^2/\lambda \approx 96.05\lambda \approx 12$ m at the chosen frequency.

We assume default power levels suitable for the selected use case: $p_{\max} = 0$ dBm, $p_{n,\max} = 3\frac{p_{\max}}{N} = \frac{p_{\max}}{48} \approx -16.81$ dBm, $\sigma_1^2 = \sigma_2^2 = -70$ dBm. The term $p_{n,\max} = 3\frac{p_{\max}}{N}$ implies that each array element can receive three times more power than if the power was equally distributed. Regarding SIC, we set $a_{\min} = 100$, which ensures that $\frac{p_2}{p_1} \geq 20$ dB. By default, we consider $\beta = 10^{-2} = 0.01$, but we also examine other values for the interference cancellation factor (Section IV-C).

We use (7) to calculate the channel vector components of $\mathbf{h}_1$ and $\mathbf{h}_2$, where $f_{i,n} = 1$ since we consider isotropic elements. For the joint optimization of the weights, $\mathbf{w}_{\text{opt}}$, and the power allocation factor, a_{opt}, we employ the SQP [33] algorithm implemented in Matlab Optimization Toolbox.[1] We set as initial values $a_0 = a_{\min} = 100$ and $\mathbf{w}_0^T = \frac{\mathbf{h}_1^H}{\|\mathbf{h}_1\|}$, which yields the upper bound of $g_{1\max}$ (Section III-B). All simulations converged in fewer than 100 iterations.

A. DIFFERENT CHANNEL CONDITIONS

In the first case, scenario #1, the locations of user 1 and user 2, $\vec{r}_i = (x_i, y_i, z_i)\lambda$, have been considered to be $\vec{r}_1 = (8, 0, 16)\lambda$ and $\vec{r}_2 = (-40, 0, 72)\lambda$, respectively. For the presented use case at 2.4 GHz, these positions translate into $\vec{r}_1 = (1, 0, 2)$ m and $\vec{r}_2 = (-5, 0, 9)$ m. Note that both users are in the antenna array NF region since their distance to the BS is less than 12 m. The norms of the corresponding channel vectors are $\|\mathbf{h}_1\| = 5.29e^{-2}$ and $\|\mathbf{h}_2\| = 1.16e^{-2}$. The beamforming gain, denoted as $g_{i,\text{BF}}$, is depicted in Fig. 2. This gain value is derived from equation (9) and represents the result after optimization in both XZ and YZ planes. Upon examining Fig. 2, it becomes clear that the optimization process enhances the beamforming gain specifically around both users. Table 1 presents the obtained values, where $R = \sqrt{R_1 R_2}$ is the geometric mean of both rates.

The proposed method is evaluated against two alternative approaches: maximizing the sum (or arithmetic mean) of the rates, by also optimizing both power allocation and beamforming (denoted as S. Max. in Table 1); and selecting maximum beamforming on user 1 while only optimizing power allocation as suggested in [22] and [23], (denoted as BF 1). In the latter case, the goal function also consists of the geometric mean of rates. Note that in this scenario where channel conditions are significantly different, maximizing the sum rate yields similar results to the product rate. However, when beamforming is focused on user 1, it marginally enhances its rate but significantly impairs user 2's rate, consequently diminishing the product rate. In every case, the power allocation factor converged to its lowest allowed value; $a_{\text{opt}} = a_{\min} = 100$. Although decreasing the value of a could potentially improve the objective function, it is assumed that

[1] https://www.mathworks.com/products/optimization.html (accessed Jan. 31, 2023)

$a = 100$ represents the minimum value that ensures SIC performance. As discussed in Section II-A, this threshold is dependent on the specific system realization and selected modulation, and it is an input parameter for the optimization process.

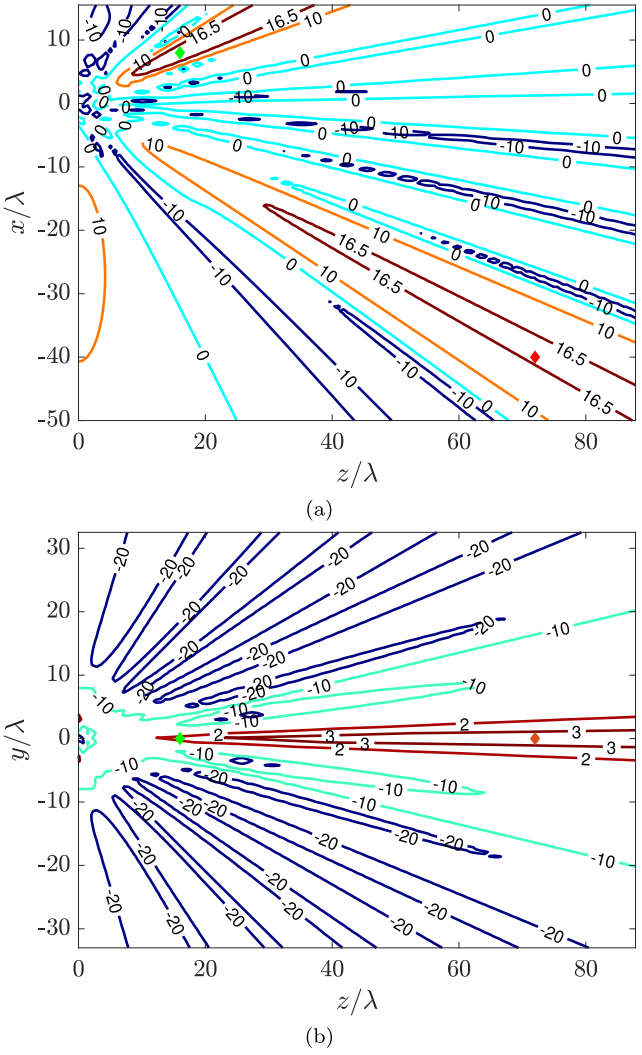

FIGURE 2. Beamforming gain (dB) for scenario #1. (a) XZ plane, (b) YZ plane. User 1 and user 2 are represented by green and red diamonds, respectively.

TABLE 1. User rates, R_i (bps/Hz); goal rate, R (bps/Hz); effective gains, g_i; and optimized power allocation factor, a_{opt}, in scenario #1. Three approaches are presented: the proposed method (Prop.), the maximization of the sum rate (S. Max.), and maximum beamforming on user 1 (BF 1).

	R	R_1	R_2	g_1	g_2	a_{opt}
Prop.	6.21	6.05	6.37	$1.88e^{-3}$	$4.51e^{-5}$	100
S. Max.	6.21	6.04	6.38	$1.85e^{-3}$	$4.53e^{-5}$	100
BF 1	0.82	6.22	0.11	$2.80e^{-3}$	$7.81e^{-9}$	100

Let us now evaluate the impact of the effective gain on the resulting capacity. Fig. 3 shows the obtained rate as a function of the effective gain for the chosen power allocation

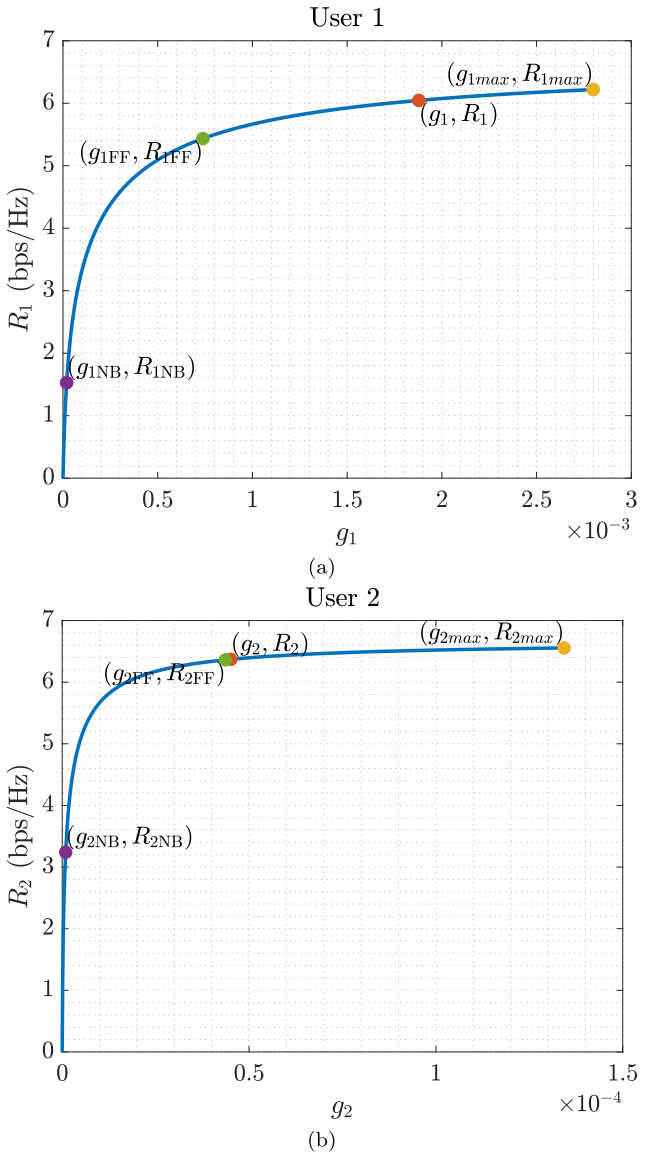

FIGURE 3. Rate as a function of the effective gain in scenario #1. (a) user 1, (b) user 2. Four points are highlighted: non-beamforming, where a single isotropic element at the origin, $\vec{r} = (0, 0, 0)$, transmits all the power, $(g_{i\text{NB}}, R_{i\text{NB}})$; the obtained effective gain using the proposed method, (g_i, R_i); the effective gain obtained not considering NF conditions in the formulation, $(g_{i\text{FF}}, R_{i\text{FF}})$; and the upper bound case, $(g_{i\text{max}}, R_{i\text{max}})$.

factor $a_{\text{opt}} = 100$, according to (5) and (10). Four points are highlighted: non-beamforming, where a single isotropic element at the origin, $\vec{r} = (0, 0, 0)$, transmits all the power, $(g_{i\text{NB}}, R_{i\text{NB}})$; the obtained effective gain using the proposed method, (g_i, R_i); the effective gain obtained not considering NF conditions in the formulation, $(g_{i\text{FF}}, R_{i\text{FF}})$; and the upper bound case, $(g_{i\text{max}}, R_{i\text{max}})$. Since we are maximizing the product of both rates, the capacity for user 2, R_2, is similar to R_1, despite having a considerably weaker channel. Moreover, the NF model improves the goal capacity, R, achieved by a formulation based on the FF approximation, $\frac{R}{R_{\text{FF}}} = 1.114$, primarily due to the increase in the rate of user 1, with $\frac{R_1}{R_{1\text{FF}}} = 1.112$, and $\frac{R_2}{R_{2\text{FF}}} = 1.001$.

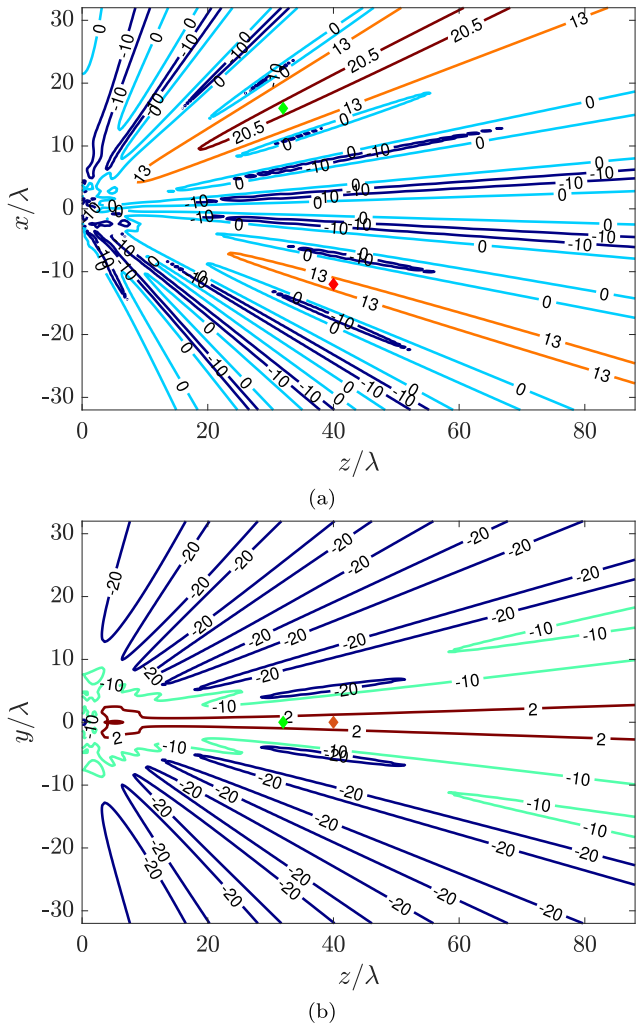

FIGURE 4. Beamforming gain (dB) for scenario #2. (a) XZ plane, (b) YZ plane. User 1 and user 2 are represented by green and red diamonds, respectively.

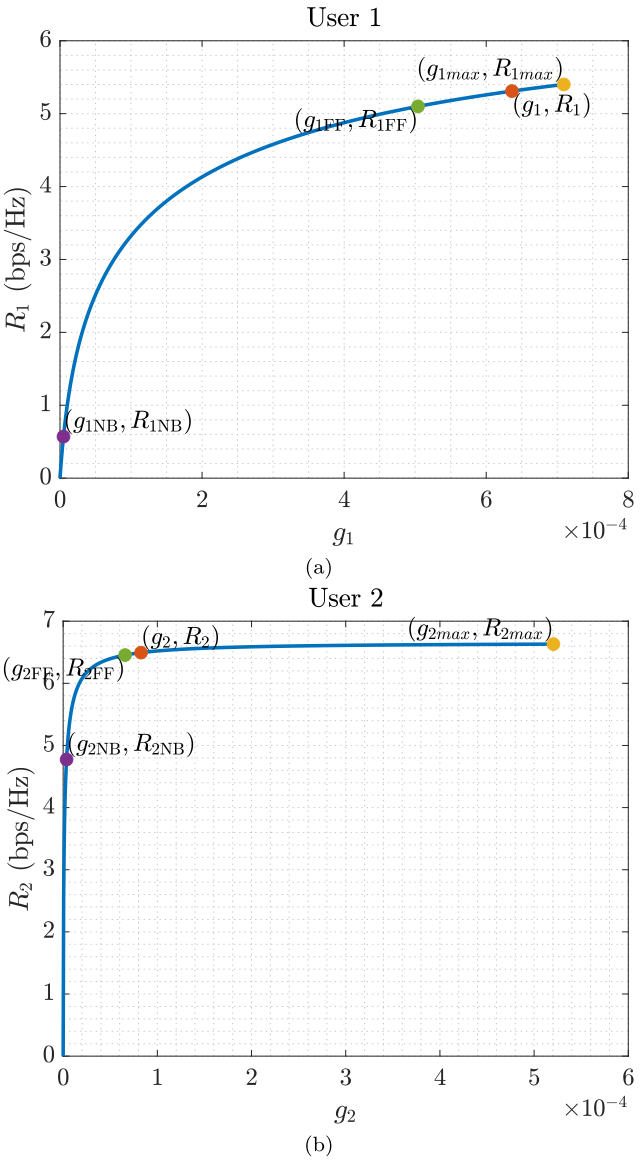

FIGURE 5. Rate as a function of the effective gain in scenario #2. (a) user 1, (b) user 2. Four points are highlighted: non-beamforming, where a single isotropic element at the origin, $\vec{r} = (0, 0, 0)$, transmits all the power, (g_{iNB}, R_{iNB}); the obtained effective gain using the proposed method, (g_i, R_i); the effective gain obtained not considering NF conditions in the formulation, (g_{iFF}, R_{iFF}); and the upper bound case, (g_{imax}, R_{imax}).

TABLE 2. User rates, R_i (bps/Hz); goal rate, R (bps/Hz); effective gains, g_i; and optimized power allocation factor, a_{opt}, in scenario #2. Three approaches are presented: the proposed method (Prop.), the maximization of the sum rate (S. Max.), and maximum beamforming on user 1 (BF 1).

	R	R_1	R_2	g_1	g_2	a_{opt}
Prop.	5.87	5.31	6.49	$6.36e^{-4}$	$8.27e^{-5}$	100
S. Max.	1.77	0.27	11.55	$1.68e^{-4}$	$5.20e^{-4}$	$7.09e^{3}$
BF 1	5.08	5.40	4.78	$7.09e^{-4}$	$3.61e^{-6}$	100

B. SIMILAR CHANNEL CONDITIONS

We now consider a case (scenario #2) where $\|\mathbf{h}_1\| \approx \|\mathbf{h}_2\|$, illustrating how applying beamforming the performance of NOMA is not affected despite keeping the $a_{\min}$ constraint. The assigned locations are now $\vec{r}_1 = (16, 0, 32)\lambda$ and $\vec{r}_2 = (-12, 0, 40)\lambda$, or $\vec{r}_1 = (2, 0, 4)$ m and $\vec{r}_2 = (-1.5, 0, 5)$ m at 2.4 GHz, which yields $\|\mathbf{h}_1\| = 2.66e^{-3}$ and $\|\mathbf{h}_2\| = 2.28e^{-3}$. As in scenario #1, both users are in the antenna array NF region.

Table 2 summarizes the obtained results for the different approaches. When compared to scenario #1 (Table 1), interesting effects can be observed. Firstly, note that for the proposed method, the power allocation factor converges to $a_{\text{opt}} = a_{\min}$, which implies that the power allocated to user 2 is 100 times higher, with $p_2 = 100\, p_1$. However, the beamforming optimization results in $g_1 = 7.7 g_2$, which limits the difference between R_1 and R_2, maintaining rate fairness. When compared to the alternative approaches already presented for scenario #1, maximum beamforming on user 1 yields a much better result in terms of rate fairness in this case, but the slight improvement in terms of R_1 compared to the proposed solution does not compensate for the degradation in R_2. Regarding the strategy of maximizing the sum

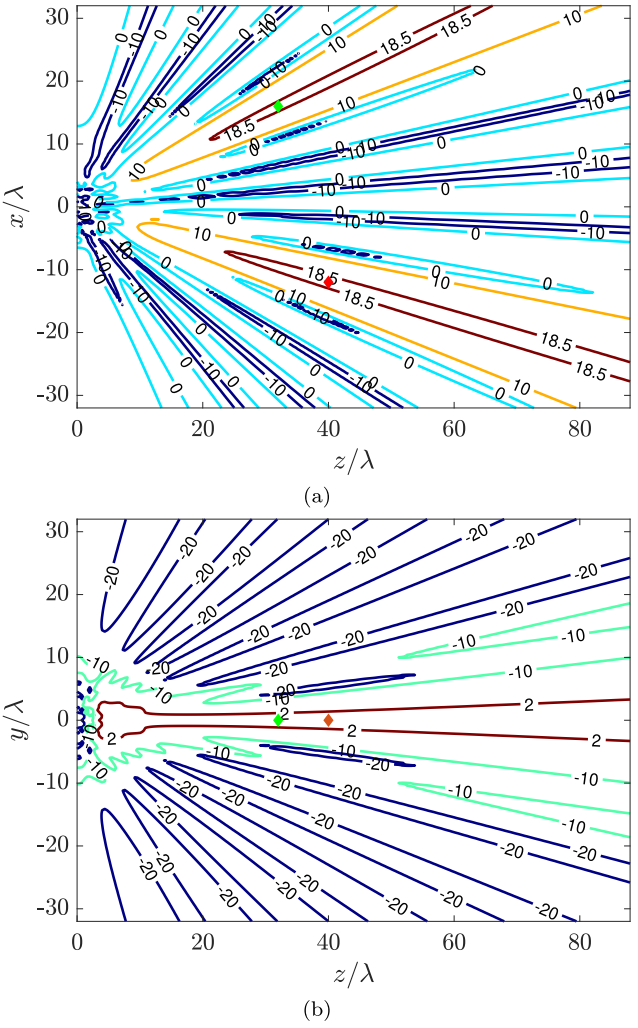

FIGURE 6. Beamforming gain (dB) for scenario #2 and TDMA. (a) XZ plane, (b) YZ plane. User 1 and user 2 are represented by green and red diamonds, respectively.

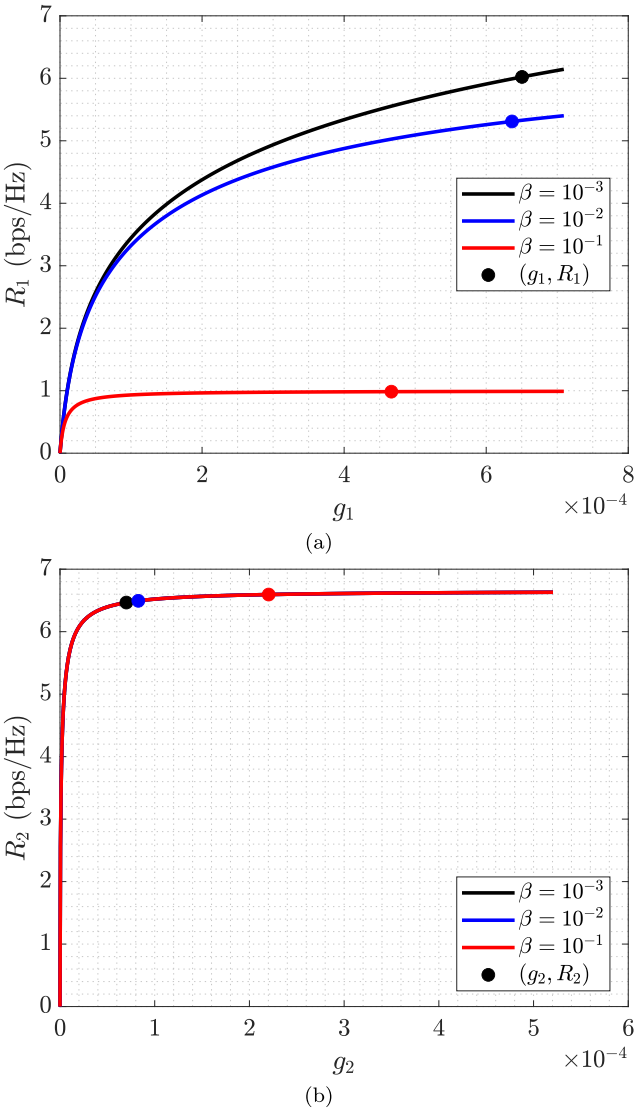

FIGURE 7. Rate as a function of the effective gain in scenario #2 for different values of β. (a) user 1, (b) user 2.

rate, most resources in terms of power and beamforming are allocated to one user at the expense of the other, as anticipated in Section II-A, and power allocation converges to $a_{\max}$.

Fig. 4 shows the resulting beamforming gain. Compared with scenario #1 (Fig. 2), the optimization focuses more on user 1 to compensate for the power allocation disparity under similar channel conditions. Fig. 5 represents the obtained rate as a function of effective gain for both users. It can be appreciated that because of the power allocation and SIC, R_1 benefits more from a higher beam factor than R_2, which is limited by interference. Consequently, the optimization algorithm brings g_1 closer to $g_{1\max}$, $\frac{g_{1\max}}{g_1} = 1.115$, than g_2 to $g_{2\max}$, $\frac{g_{2\max}}{g_2} = 6.289$. Similarly, in the case of beamforming not being applied, the impact is significantly stronger on user 1 than on user 2 since the former compensates a lower effective gain with the greater allocated power, being $\frac{R_1}{R_{1\mathrm{NB}}} = 10.526$, and $\frac{R_2}{R_{2\mathrm{NB}}} = 1.355$. Comparison between NF and FF models for this case yields $\frac{R}{R_{\mathrm{FF}}} = 1.048$, with $\frac{R_1}{R_{1\mathrm{FF}}} = 1.041$, and $\frac{R_2}{R_{2\mathrm{FF}}} = 1.006$, justifying again the use of NF formulation for this scenario.

C. COMPARISON WITH TDMA

No matter the channel conditions, a measure for evaluating the performance of NOMA is to compare it against another MA strategy. We compare the proposed approach with the obtained results using TDMA [35] for the same problem. To make a fair comparison, we also applied beamforming for the TDMA case and the same optimization algorithm (without power allocation) to find the optimal weights that maximize the product rate. In TDMA, only one user is served at a time with all available power, p_{max}. The resulting capacity rate for the i-th user, $R_{i_{\mathrm{TDMA}}}$, can be expressed as

$$R_{i_{\mathrm{TDMA}}} = \log_2\left(1 + \frac{p_{\max} g_i}{\sigma_{n_i}^2}\right)\alpha_i \tag{14}$$

where g_i denotes the effective gain of the array as expressed in (6); and α_i the timeslot allocation factor for the i-th user, or the time fraction during which user is served. Assuming

instantaneous multiplex $\alpha_1+\alpha_2 = 1$. For the sake of comparison, we consider $\alpha_1 = \alpha_2 = 0.5$. Fig. 6 shows the resulting beamforming gain that TDMA adopts in scenario #2. Compared with Fig. 4, beamforming results in a lower gain for user 1, since there is no need to compensate for the differences in the allocated power.

Table 3 and Table 4 represent the results for scenario #1 and scenario #2, respectively. Results show that NOMA outperforms TDMA in terms of the product rate when $\beta \leq 10^{-2}$. For $\beta = 10^{-2}$, NOMA is better in scenario #1, and both strategies yield similar results in scenario #2. In the case of $\beta = 10^{-1}$, user 1 is severely limited by imperfect SIC, and the optimization algorithm focuses on maintaining the capacity for user #2. This confirms that NOMA performance is highly dependent on the cancellation factor.

An interesting effect is that, although R always decreases when β increases, sometimes there is a marginal improvement in R_2 at the expense of R_1 (see Table 4). User 1 is more limited by interference with higher values of β, which makes the optimization algorithm spend fewer resources on yielding a high value for g_1. Fig. 7 shows the rate as a function of the beam factor in scenario #2 for different values of β. Note that the rate of user 2 is slightly affected when β changes, although it is not included in R_2 as expressed in (5). This is because the optimization algorithm yields different values of the allocated power, p_2, and effective gain, g_2, depending on the scenario.

TABLE 3. Comparison between NOMA and TDMA obtained rates, in bps/Hz, for scenario #1.

	TDMA	NOMA		
		$\beta = 10^{-3}$	$\beta = 10^{-2}$	$\beta = 10^{-1}$
R	5.70	6.95	6.21	2.54
R_1	6.76	7.69	6.05	0.99
R_2	4.81	6.28	6.37	6.51

TABLE 4. Comparison between NOMA and TDMA obtained rates, in bps/Hz, for scenario #2.

	TDMA	NOMA		
		$\beta = 10^{-3}$	$\beta = 10^{-2}$	$\beta = 10^{-1}$
R	5.84	6.24	5.87	2.55
R_1	5.94	6.02	5.31	0.98
R_2	5.74	6.47	6.49	6.59

V. CONCLUSION

In this paper, we have studied the application of beamforming in a two-user MISO downlink NOMA system, taking into account the effect of imperfect SIC and showing how our solution can overcome the limitation of SISO NOMA in terms of rate fairness when the channels to both users are similar. Furthermore, we use an antenna model that considers NF radiation. NF conditions can be found in picocells or femtocells depending on the antenna and frequency, which in this paper is exemplified with a use case.

We initially derived the problem formulation and identified the challenge in NOMA of achieving similar rates for users with similar channel conditions. The joint optimization of the power allocation and the weights of the array yields a non-convex problem with non-linear constraints that we have solved using the SQP algorithm. The proposed model directly yields the complex weights to configure a specific array characterized by its geometry and the radiation pattern of its elements, which highly enhances its applicability in a real-life use case. In order to enhance rate fairness, we have maximized the geometric mean of the rates, which avoids the typical effect of an overall high rate due to an uneven split of resources in favour of one user at the expense of the other.

We have simulated a typical NOMA scenario, where the user performing SIC has a stronger channel and another one with similar channel conditions for both users. Results show that both users benefit from beamforming and obtain similar rates in every case. Furthermore, the proposed method has demonstrated better performance compared to two alternative approaches: one that maximizes the sum rate, and another that yields maximum beamforming to the user that is allocated less power. Finally, a comparison with beamforming TDMA shows that, given a sufficient level of interference cancellation, beamforming NOMA can yield higher rates in a MISO case even when aiming for rate fairness, similar channel conditions, and keeping the power allocation constraints that ensure SIC performance.

REFERENCES

[1] Z. Ding, X. Lei, G. K. Karagiannidis, R. Schober, J. Yuan, and V. K. Bhargava, "A survey on non-orthogonal multiple access for 5G networks: Research challenges and future trends," *IEEE J. Sel. Areas Commun.*, vol. 35, no. 10, pp. 2181–2195, Oct. 2017.

[2] Y. Saito, A. Benjebbour, Y. Kishiyama, and T. Nakamura, "System-level performance evaluation of downlink non-orthogonal multiple access (NOMA)," in *Proc. IEEE 24th Annu. Int. Symp. Pers., Indoor, Mobile Radio Commun. (PIMRC)*, Sep. 2013, pp. 611–615.

[3] Z. Ding, Z. Yang, P. Fan, and H. V. Poor, "On the performance of non-orthogonal multiple access in 5G systems with randomly deployed users," *IEEE Signal Process. Lett.*, vol. 21, no. 12, pp. 1501–1505, Dec. 2014.

[4] J. Choi, "On generalized downlink beamforming with NOMA," *J. Commun. Netw.*, vol. 19, no. 4, pp. 319–328, Aug. 2017.

[5] M. F. Hanif, Z. Ding, T. Ratnarajah, and G. K. Karagiannidis, "A minorization-maximization method for optimizing sum rate in the downlink of non-orthogonal multiple access systems," *IEEE Trans. Signal Process.*, vol. 64, no. 1, pp. 76–88, Jan. 2016.

[6] Z. Xiao, L. Zhu, J. Choi, P. Xia, and X. Xia, "Joint power allocation and beamforming for non-orthogonal multiple access (NOMA) in 5G millimeter wave communications," *IEEE Trans. Wireless Commun.*, vol. 17, no. 5, pp. 2961–2974, May 2018.

[7] L. Pang, W. Wu, Y. Zhang, Y. Yuan, Y. Chen, A. Wang, and J. Li, "Joint power allocation and hybrid beamforming for downlink mmWave-NOMA systems," *IEEE Trans. Veh. Technol.*, vol. 70, no. 10, pp. 10173–10184, Oct. 2021.

[8] L. Zhu, J. Zhang, Z. Xiao, X. Cao, D. O. Wu, and X. Xia, "Joint power control and beamforming for uplink non-orthogonal multiple access in 5G millimeter-wave communications," *IEEE Trans. Wireless Commun.*, vol. 17, no. 9, pp. 6177–6189, Sep. 2018.

[9] M. Zeng, W. Hao, A. Yadav, N. Nguyen, O. A. Dobre, and H. V. Poor, "Energy-efficient joint power control and receiver design for uplink mmWave-NOMA," in *Proc. IEEE Int. Conf. Commun. Workshops (ICC Workshops)*, Jun. 2020, pp. 1–5.

[10] Y. Fu, M. Zhang, L. Salaün, C. W. Sung, and C. S. Chen, "Zero-forcing oriented power minimization for multi-cell MISO-NOMA systems: A joint user grouping, beamforming, and power control perspective," *IEEE J. Sel. Areas Commun.*, vol. 38, no. 8, pp. 1925–1940, Aug. 2020.

[11] Z. Xiao, L. Zhu, Z. Gao, D. O. Wu, and X. Xia, "User fairness non-orthogonal multiple access (NOMA) for millimeter-wave communications with analog beamforming," *IEEE Trans. Wireless Commun.*, vol. 18, no. 7, pp. 3411–3423, Jul. 2019.

[12] L. Zhu, J. Zhang, Z. Xiao, X. Cao, D. O. Wu, and X. Xia, "Millimeter-wave NOMA with user grouping, power allocation and hybrid beamforming," *IEEE Trans. Wireless Commun.*, vol. 18, no. 11, pp. 5065–5079, Nov. 2019.

[13] M. R. G. Aghdam, B. M. Tazehkand, and R. Abdolee, "Joint optimal power allocation and beamforming for MIMO-NOMA in mmWave communications," *IEEE Wireless Commun. Lett.*, vol. 11, no. 5, pp. 938–941, May 2022.

[14] I. Abu Mahady, E. Bedeer, S. Ikki, and H. Yanikomeroglu, "Sum-rate maximization of NOMA systems under imperfect successive interference cancellation," *IEEE Commun. Lett.*, vol. 23, no. 3, pp. 474–477, Mar. 2019.

[15] Y. Saito, Y. Kishiyama, A. Benjebbour, T. Nakamura, A. Li, and K. Higuchi, "Non-orthogonal multiple access (NOMA) for cellular future radio access," in *Proc. IEEE 77th Veh. Technol. Conf. (VTC Spring)*, Jun. 2013, pp. 1–5.

[16] Y. Yu, H. Chen, Y. Li, Z. Ding, L. Song, and B. Vucetic, "Antenna selection for MIMO nonorthogonal multiple access systems," *IEEE Trans. Veh. Technol.*, vol. 67, no. 4, pp. 3158–3171, Apr. 2018.

[17] Z. Ding, P. Fan, and H. V. Poor, "Impact of user pairing on 5G nonorthogonal multiple-access downlink transmissions," *IEEE Trans. Veh. Technol.*, vol. 65, no. 8, pp. 6010–6023, Aug. 2016.

[18] N. S. Mouni, A. Kumar, and P. K. Upadhyay, "Adaptive user pairing for NOMA systems with imperfect SIC," *IEEE Wireless Commun. Lett.*, vol. 10, no. 7, pp. 1547–1551, Jul. 2021.

[19] S. Timotheou and I. Krikidis, "Fairness for non-orthogonal multiple access in 5G systems," *IEEE Signal Process. Lett.*, vol. 22, no. 10, pp. 1647–1651, Oct. 2015.

[20] J. Álvarez, R. Ayestarán, and F. Las-Heras, "Design of antenna arrays for near-field focusing requirements using optimisation," *IET Electron. Lett.*, vol. 48, no. 21, pp. 1323–1325, 2012.

[21] A. Buffi, P. Nepa, and G. Manara, "Design criteria for near-field-focused planar arrays," *IEEE Antennas Propag. Mag.*, vol. 54, no. 1, pp. 40–50, Feb. 2012.

[22] Z. Ding, L. Dai, and H. V. Poor, "MIMO-NOMA design for small packet transmission in the Internet of Things," *IEEE Access*, vol. 4, pp. 1393–1405, 2016.

[23] Z. Ding, Z. Zhao, M. Peng, and H. V. Poor, "On the spectral efficiency and security enhancements of NOMA assisted multicast-unicast streaming," *IEEE Trans. Commun.*, vol. 65, no. 7, pp. 3151–3163, Jul. 2017.

[24] F. D. Neeser and J. L. Massey, "Proper complex random processes with applications to information theory," *IEEE Trans. Inf. Theory*, vol. 39, no. 4, pp. 1293–1302, Jul. 1993.

[25] A. Agrawal, J. G. Andrews, J. M. Cioffi, and T. Meng, "Iterative power control for imperfect successive interference cancellation," *IEEE Trans. Wireless Commun.*, vol. 4, no. 3, pp. 878–884, May 2005.

[26] Y. Iraqi and A. Al-Dweik, "Power allocation for reliable SIC detection of rectangular QAM-based NOMA systems," *IEEE Trans. Veh. Technol.*, vol. 70, no. 8, pp. 8355–8360, Aug. 2021.

[27] K. Ferdi and K. Hakan, "A true power allocation constraint for non-orthogonal multiple access with M-QAM signalling," in *Proc. IEEE Microw. Theory Techn. Wireless Commun.*, vol. 1, Oct. 2020, pp. 7–12.

[28] M. R. Pino, R. G. Ayestarán, P. Nepa, and G. Manara, "An overview on synthesis techniques for near-field focused antennas," in *Recent Wireless Power Transfer Technologies*, P. Pinho, Ed. Rijeka, Croatia: IntechOpen, 2019, ch. 1.

[29] A. Goldsmith, "Path loss and shadowing," in *Wireless Communications*. Cambridge, U.K.: Cambridge Univ. Press, 2004, ch. 2, pp. 31–33.

[30] J. Á. Muñiz, R. G. Ayestarán, J. Laviada, and F. Las-Heras, "Support vector regression for near-field multifocused antenna arrays considering mutual coupling," *Int. J. Numer. Modelling: Electron. Netw., Devices Fields*, vol. 29, no. 2, pp. 146–156, Mar. 2016.

[31] C. A. Balanis, "Fundamental parameters and figures-of-merit of antennas," in *Antenna Theory: Analysis and Design*, 4th ed. Hoboken, NJ, USA: Wiley, 2016, ch. 2, pp. 25–35.

[32] J. Nocedal and S. J. Wright, "Theory of constrained optimization," in *Numerical Optimization*, 2nd ed. New York, NY, USA: Springer, 2006, ch. 12, pp. 304–351.

[33] J. Nocedal and S. J. Wright, "Sequential quadratic programming," in *Numerical Optimization*, 2nd ed. New York, NY, USA: Springer, 2006, ch. 18, pp. 529–561.

[34] A. Goldsmith, "Multiple antennas and space-time communications," in *Wireless Communications*. Cambridge, U.K.: Cambridge Univ. Press, 2004, ch. 10, pp. 334–335.

[35] A. Goldsmith, "Multiuser systems," in *Wireless Communications*. Cambridge, U.K.: Cambridge Univ. Press, 2004, ch. 14, pp. 454–461.

ÁLVARO PENDÁS-RECONDO received the B.Sc. and M.Sc. degrees in telecommunications engineering from the University of Oviedo, Gijón, Spain, in 2019 and 2021, respectively, where he is currently pursuing the Ph.D. degree.

He has been an Intern with the NASA Jet Propulsion Laboratory (JPL), Microwave Instrument Science Group, Pasadena, CA, USA, in the summer of 2019; German Aerospace Center (DLR) Institute of Communications and Navigation, Oberpfaffenhofen, Germany, in the summer of 2020; and with the Research and Innovation Department, Rakuten Mobile Inc., Tokyo, Japan, in 2022. Since 2019, he has been a Research Assistant with the Group of Signal Theory and Communications, University of Oviedo. His research interests include information theory and signal processing applied to multiuser wireless communications.

RAFAEL GONZÁLEZ AYESTARÁN (Senior Member, IEEE) received the B.Tech. and Telecommunication Engineering degrees from the University of Cantabria, Spain, in 1995 and 1997, respectively, and the Ph.D. degree from the University of Oviedo, Spain, in 2004.

From 1997 to 2001, he was with the Department of Communications Engineering, University of Cantabria. In 2001, he joined the Department of Electrical Engineering, University of Oviedo, where he is currently the Deputy Head. Since 2020, he has been the holder of the THIN5G Chair of the University of Oviedo, supported by the Government of the Principality of Asturias. His research interests include digital signal processing, digital communications, machine learning, and computational methods and their application to communications and electromagnetic problems.

JESÚS ALBERTO LÓPEZ-FERNÁNDEZ was born in Avilés, Asturias, Spain. He received the M.Sc. and Ph.D. degrees in telecommunication engineering from the University of Vigo, Spain, in 1999 and 2009, respectively.

From April 2002 to March 2003, he was a Marie-Curie Visiting Fellow with the Mechanical and Manufacturing Engineering Department, Trinity College Dublin (TCD). Since October 2003, he has been with the Electrical Engineering Department, University of Oviedo, Asturias, where he is currently an Associate Professor, teaching courses on digital communications and radar systems. His research interests include iterative methods and speed-up schemes, parallel algorithms, machine learning, and signal processing.